Fifth Aerodynamics Prediction Challenge (APC-V)
2018/07/01, Tokyo

Steady Aerodynamic Prediction of 30P30N Using Hierarchical Cartesian Mesh and Adaptive Mesh Refinement

○ SHU Kembun, SUGAYA Keisuke, IMAMURA Taro
(The University of Tokyo)

YOSHIHARA Tamaki
(Tohoku University)

東京大学
THE UNIVERSITY OF TOKYO

Background

- UTCart (The University of Tokyo Cartesian grid based automatic flow solver)
- Hierarchical Cartesian Mesh
  - ✓ Automatic, rapid, robust grid generation.
  - ✓ Easy to local refining.
  - ✓ The Immersed Boundary Method with a wall function[1].

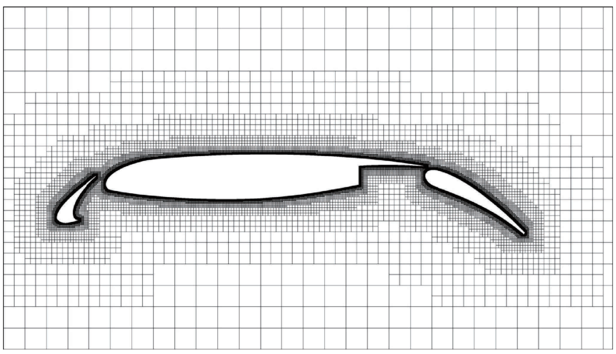

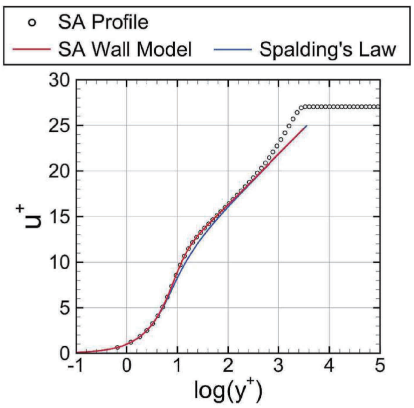

1) Tamaki, and Imamura, AIAA J., Vol 56, 2018

Background

- ➢Making proper grid for HLD analysis is still difficult.
  - ✓Low grid resolution in wake region, far region
    - Compared to structured body-fitted grid[1)]
    - Cause inferior aerodynamic prediction ability?
  - ✓Manual control require users' experiment.

⇒ **Solution-Adaptive Mesh Refinement (AMR)**

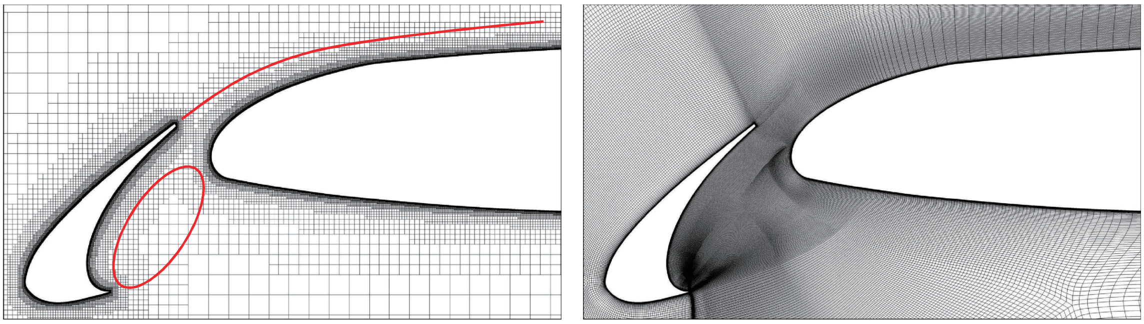

1) https://cfdws.chofu.jaxa.jp/apc/external/2D_domain.tar.gz

Objective

- ➢AMR capability on HLD analysis is examined.
  - ✓**Influence on aerodynamic prediction ability**
- ➢Case 1-1 (2D steady flow)
- ➢Updates from APC-IV
  - ✓Dependency of refined region is examined.
    - Wake region or acceleration/deceleration region?
  - ✓Necessity of AMR is discussed.

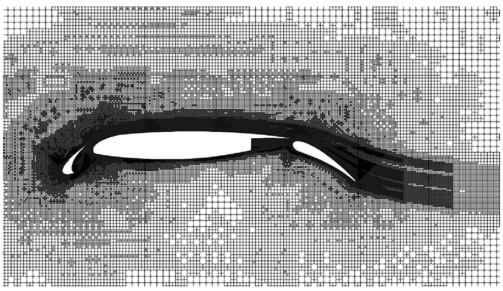

AMR grid from APC-IV

Analysis workflow

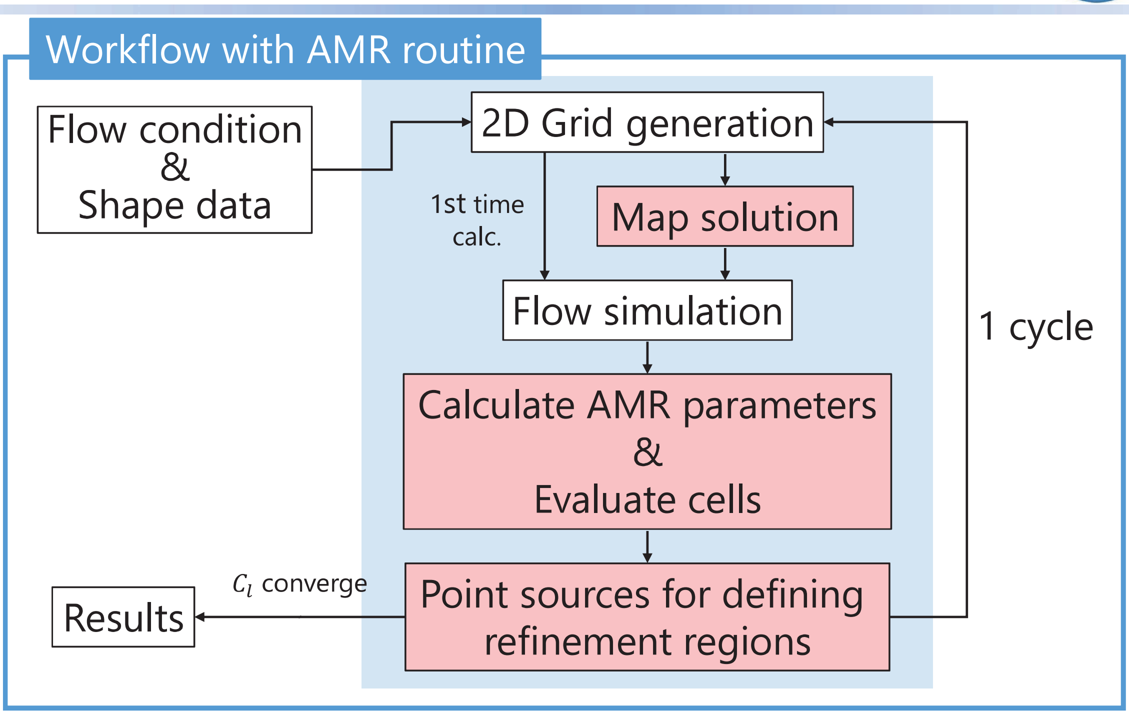

5

Analysis workflow

Calculate AMR parameters & Evaluate cells

Feature-based parameters[1, 2)]

$$\tau_C = |\nabla \cdot \vec{u}| h^{\frac{3}{2}} \quad \text{Compressibility}$$

$$\tau_R = |\nabla \times \vec{u}| h^{\frac{3}{2}} \quad \text{Rotation}$$

$$\tau_E = \left| \nabla \frac{1}{\gamma - 1} \ln \left[\frac{p}{p_\infty} \left(\frac{\rho_\infty}{\rho} \right)^{\gamma} \right] \right| h^{\frac{3}{2}} \quad \text{Entropy}$$

$$\sigma_i = \sqrt{\sum_{j=1}^{N} \frac{\tau_{i_j}}{N}} \quad (i = C, R, E)$$

h : Cell size
N : Total cell #

Map solution

- $\tau_i > \sigma_i$
→ Refinement

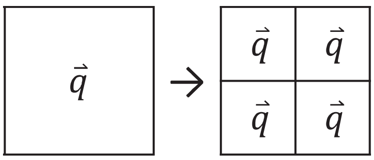

- $\tau_i < 0.1\sigma_i$
→ Coarsening

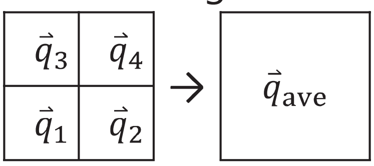

1) De Zeeuw, D. *et al.* AIAA Paper 92-0321.
2) Hartmann, D. *et al.* Computers & Fluids, 2008.

6

Numerical method & conditions

- Governing equations : 2D RANS
- Turbulence model : SA-noft2
- Wall boundary condition : Immersed boundary method +SA wall model[1)]
- Time integration : LU-SGS
- Spatial accuracy (Inviscid) : 4th order upwind-biased scheme[2)]
- Spatial accuracy (Viscous) : 2nd order central difference

1) Tamaki, and Imamura, AIAA J., Vol 56, 2018.
2) 玉置, and 今村, ながれ33, 2014

7

Computational grids

- Unstructured Cartesian grid
- Domain size : $56.9C_{\mathrm{ref}} \times 56.9C_{\mathrm{ref}}$
- Minimum cell size : $1.09 \times 10^{-4}C_{\mathrm{ref}}$ $(y^{+}_{\mathrm{IP}} \leq 60)$

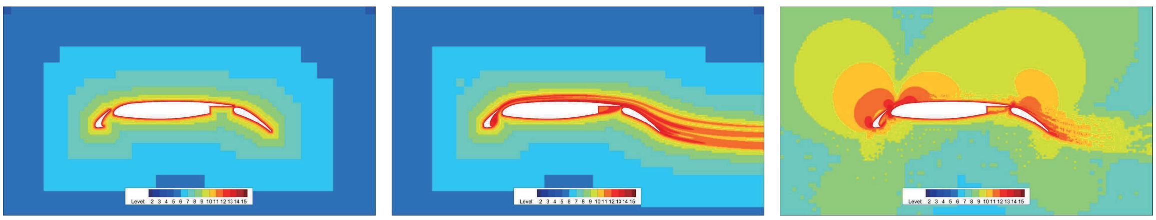

Initial grid
212,367 cell

Wake-detected grid
Using τ_R, τ_E
~400k cell

DivV-detected grid
Using τ_C
~350k cell

AMR grids

Colored by cell level distribution
$\Delta x = \Delta x_{max} \times 1/2^{level}$

8

AMR history (AoA 9.5 deg, Wake)

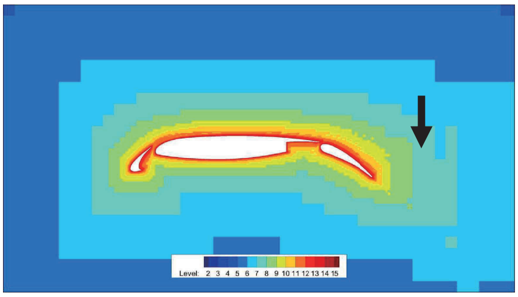

1 cycle: 239k cell

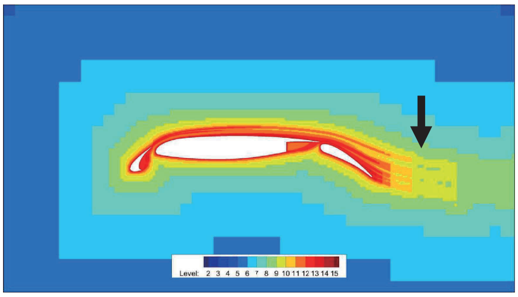

3 cycle: 304k cell

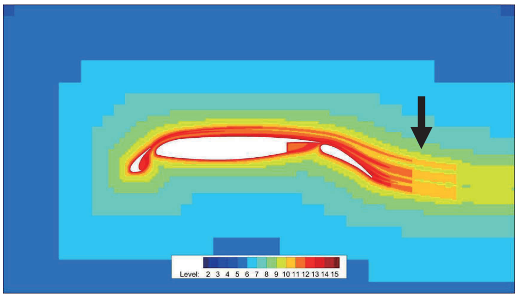

4 cycle: 353k cell

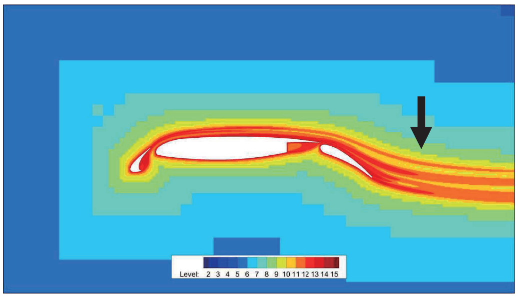

6 cycle: 404k cell

AMR history (AoA 9.5 deg, Wake)

- Wake regions are successfully refined.
  - ✓ Slat cusp, slat wake, flap wake
- Boundary layer is also refined.

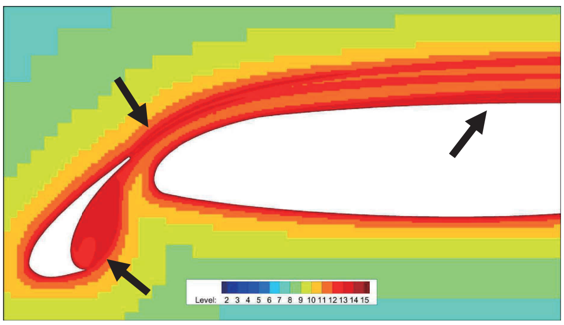

Slat

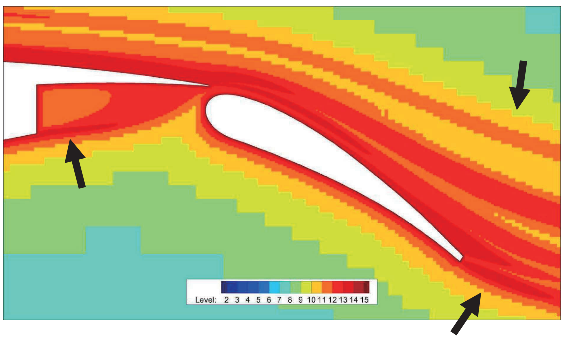

Flap

6 cycle grid

AMR history (AoA 9.5 deg, DivV)

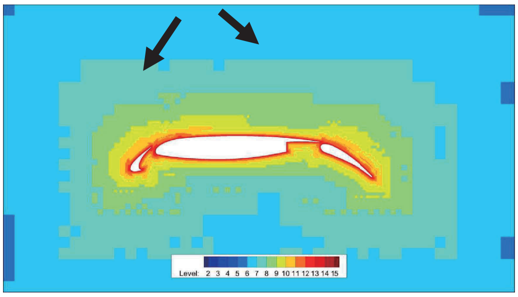

1 cycle: 226k cell

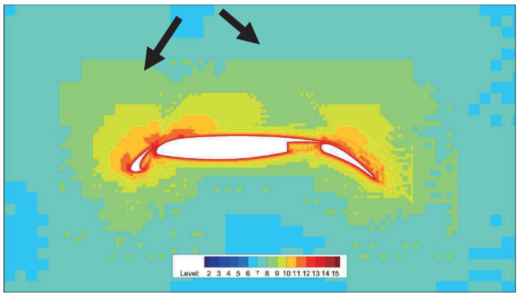

2 cycle: 254k cell

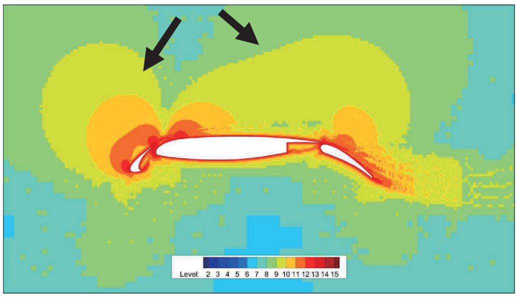

4 cycle: 325k cell

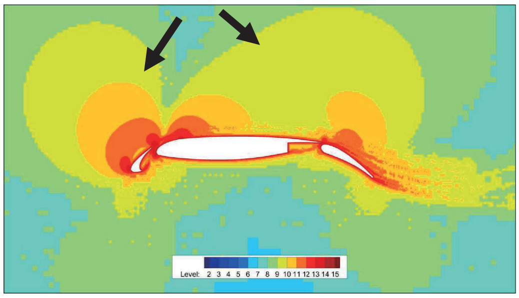

5 cycle: 373k cell

11

AMR history (AoA 9.5 deg, DivV)

- Acceleration/deceleration regions are refined.
  - ✓ Gap between slat-main, main-flap
  - ✓ Leading edge of each element
- Wake regions are also refined slightly.
  - ✓ Due to the velocity variation

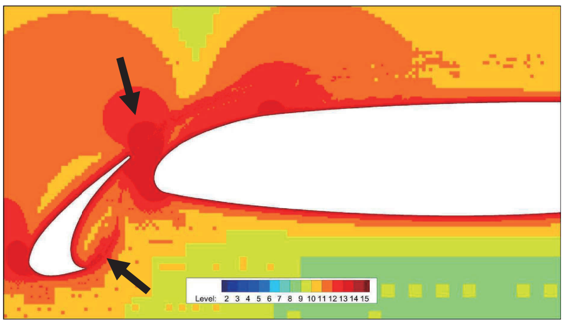

Slat

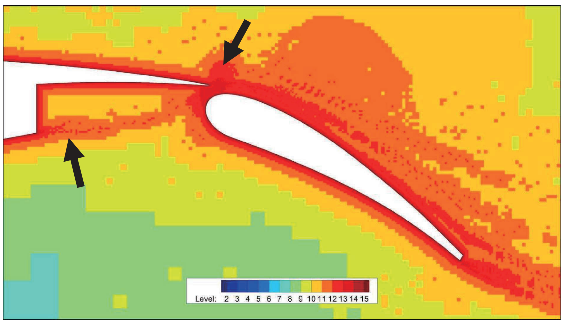

Flap

5 cycle grid

12

C_l–AoA curve

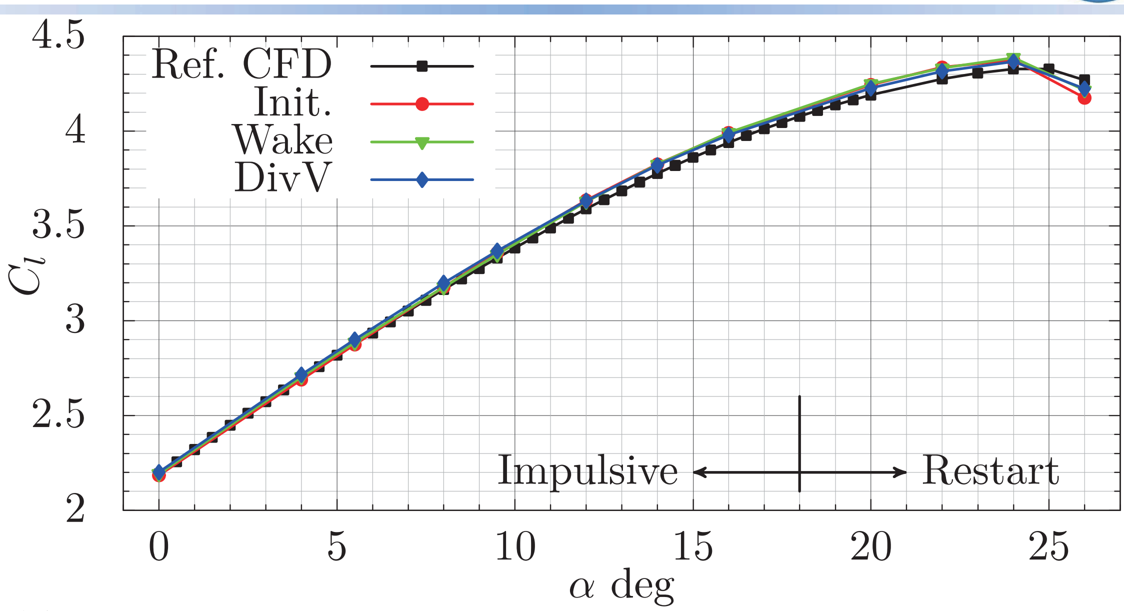

※ In AoA ≥ 20 deg, calculation is restarted using previous AoAs' flow field.

cf. Appendix

Ref. CFD: Murayama *et al.*, AIAA 2018-3460, 2018

13

C_l difference between each grid

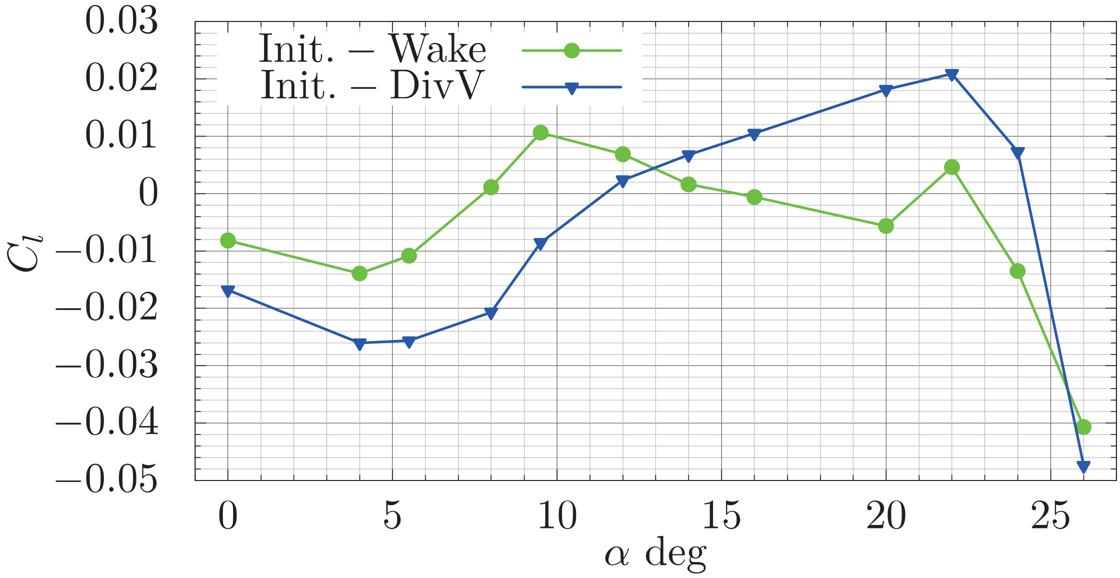

- Absolute of C_l variation is ≤ 0.05.
- No drastic difference is seen between Wake and DivV.

14

C_d–AoA curve

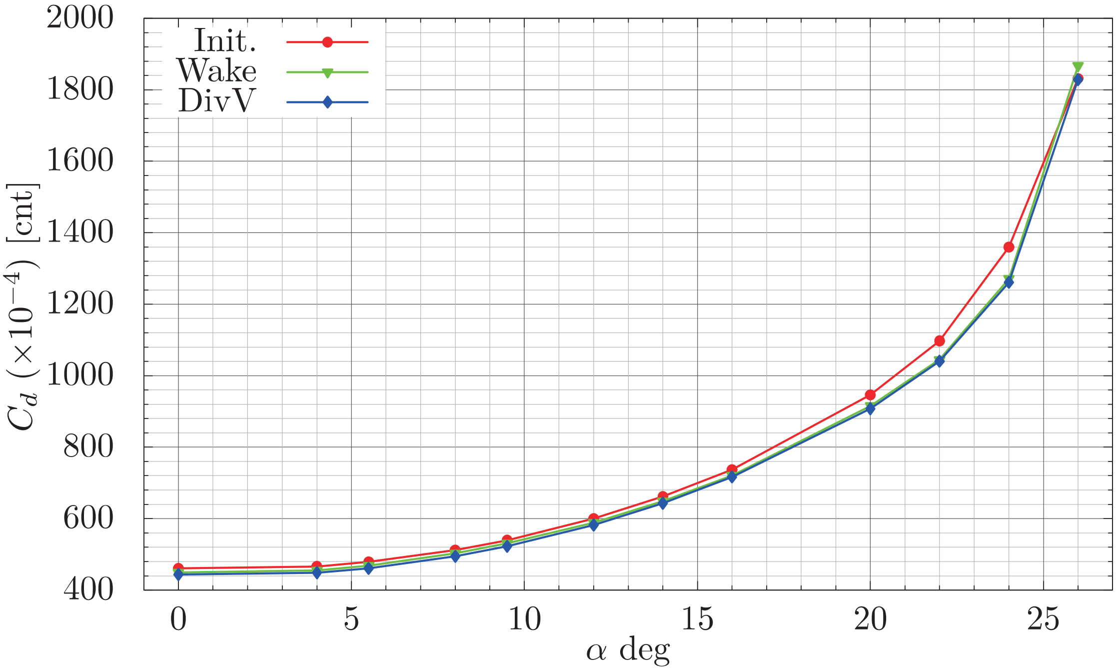

➢ C_d variation is ≤ 20 cnt.

15

C_d difference between each grid

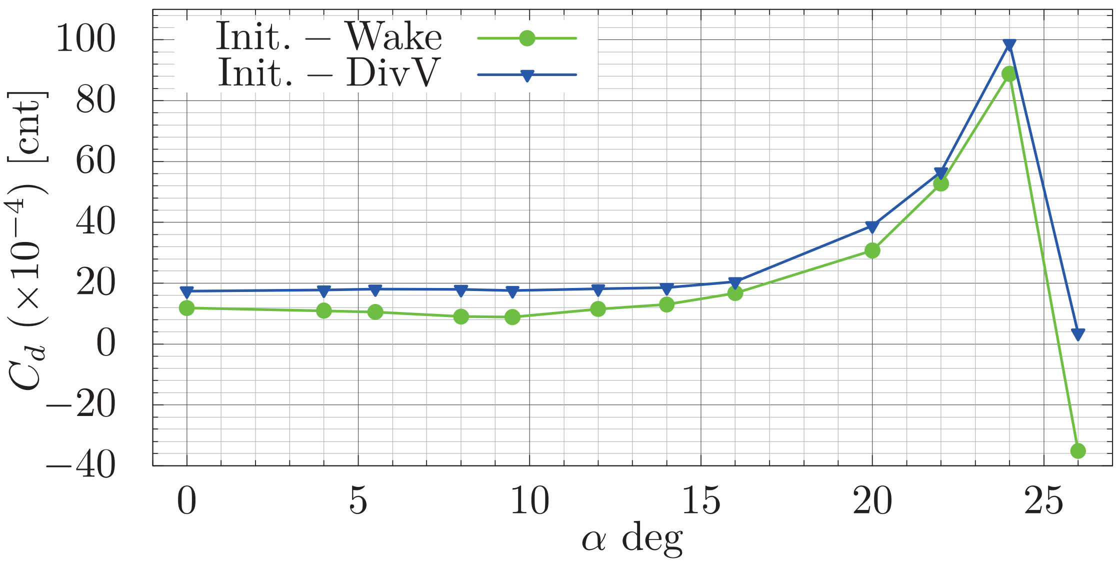

➢ Absolute of C_d variation is about 20 cnt.

- ✓ Large in AoA ≥ 20 deg.

➢ DivV has larger influence than Wake.

16

Velocity profile at AoA=5.5 deg

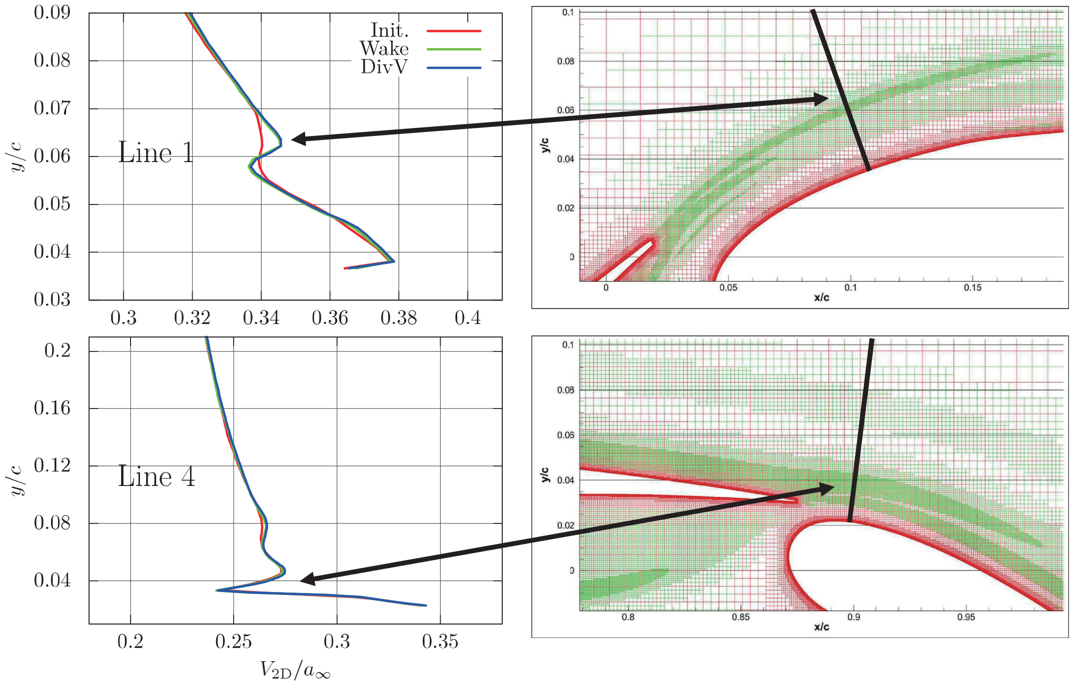

➢Wake resolution is improved slightly in some regions.

When is AMR useful?

✗ To avoid separation, AMR is not necessarily needed.
  - ✓Restart from lower AoA is sufficient.

✗ C_l can be calculated with accuracy of ≤ 0.05 without AMR.

◯ C_d can be affected by ~20 cnt using AMR.
  - ✓DivV region is dominant rather than wake region.

◯ For objective to capture wake, shear layer.

Conclusions

- ➢Steady flow simulation was conducted by UTCart.
  - ✓Feature-based AMR controlled spatial resolution automatically.
- ➢Wake-detected grid and velocity variation-detected grid were compared.
  - ✓C_l did not differ larger than 0.05 between each grid.
  - ✓C_d was affected by ~20 cnt using variation-detected grid.
  - ✓Wake resolution can be improved.

19

Appendix; impulsive start in high AoA

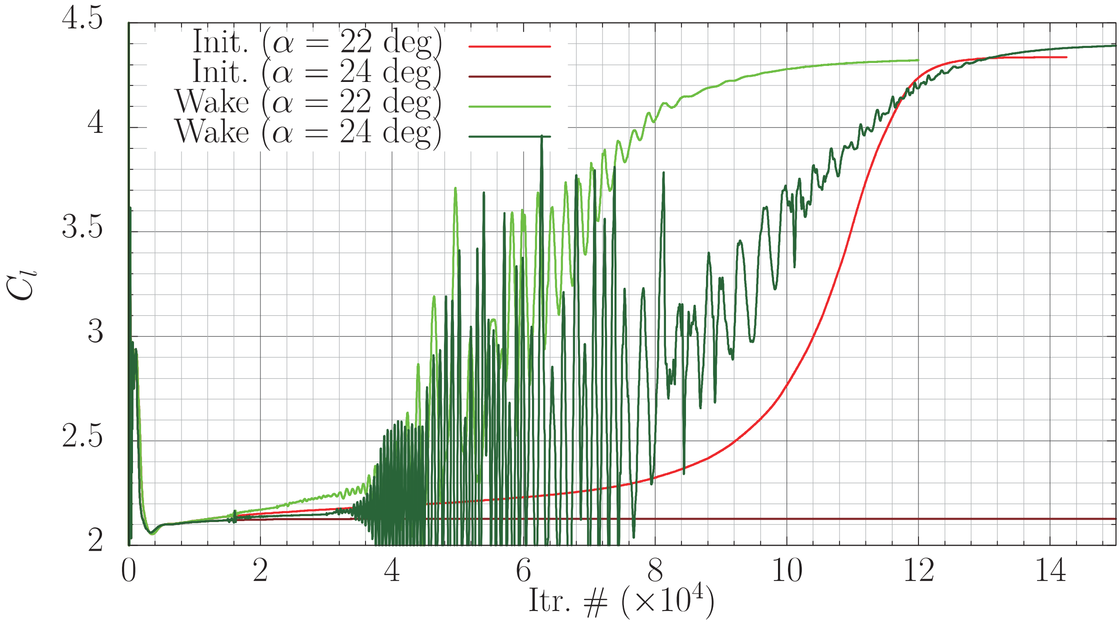

- ➢Impulsive start in high AoAs require much Itr. # to get flow attached (AoA 22 deg), or flow never attach (AoA 24 deg).

20

Appendix; wake, 3rd or 4th order?

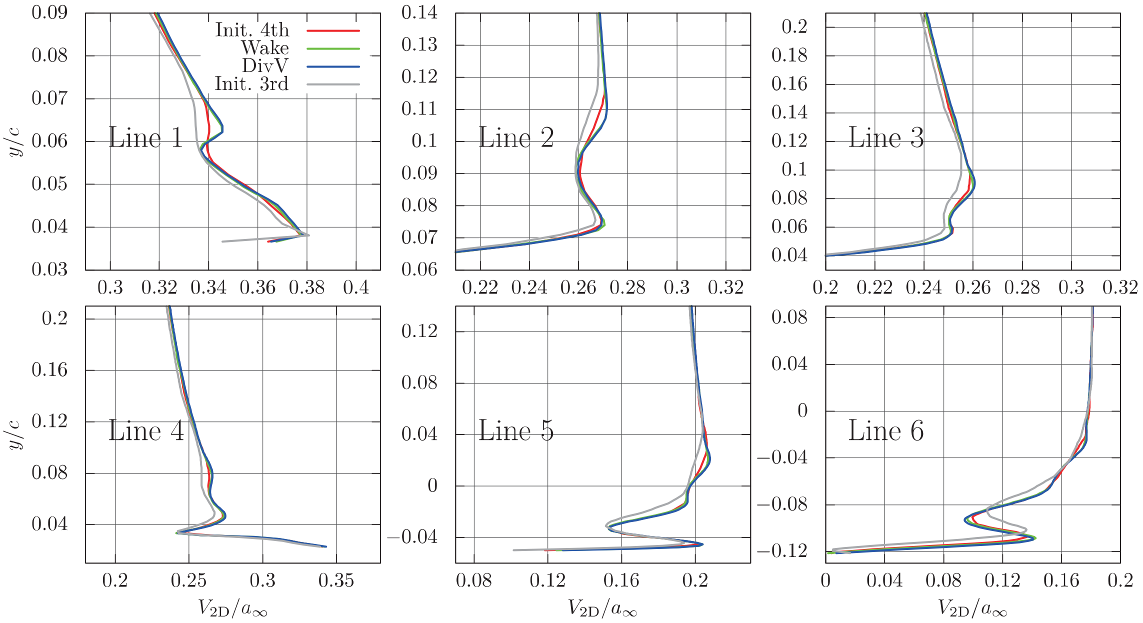

- Wake resolution by 3rd order scheme is inferior to others'.
  - ✓ High wake resolution seen in Init. grid is due to 4th order scheme.

21